Multi-Time Scale Optimal Scheduling of Regional Integrated Energy Systems Considering Integrated Demand Response

HAIZHU YANG[1], MENGLONG LI[ID][1], ZHAOYANG JIANG[1], AND PENG ZHANG[2]

[1]School of Electrical Engineering and Automation, Henan Polytechnic University, Jiaozuo 454000, China
[2]School of Electrical and Information Engineering, Tianjin University, Tianjin 300072, China

Corresponding author: Menglong Li (melonlee0188@163.com)

ABSTRACT The regional integrated energy system (RIES) is an important place for energy development such as multi-energy complementarities and energy Internet, RIES has important application value for realizing sustainable energy development and building a lower-carbon society, the dissipation of renewable energy and the stabilization of load fluctuations have brought challenges to its optimal operation. Integrated demand response (IDR) is detailedly described by price-based and alternative response. Establish a day-ahead and intraday optimization scheduling model considering the demand side response. According to the difference of scheduling time of each energy subsystem of electric, cooling/heating and natural gas, it is divided into three sub-layers of slow control, intermediate control and fast control to perform rolling optimization scheduling. The example analysis shows that the multi-time scale optimization scheduling model can meet the supply and demand balance of the system, and can also restrain the fluctuation of renewable energy and load intraday, improve the stability of the system, and further reduce the operating cost of the system.

INDEX TERMS Regional integrated energy system, integrated demand response, multi-time scale, intraday optimal, the minimum cost of scheduling.

I. INTRODUCTION

The fossil energy crisis and environmental pollution are serious problems. Vigorously developing renewable energy and improving energy efficiency have become inevitable choices for sustainable energy development [1]–[5]. The RIES is a modern energy system that integrates cooling/heating and natural gas systems with the electrical power system as the core, and it is the focus of research [6]. Demand side response can guide users to use energy rationally, reasonable transfer of peak energy consumption to stabilize peak and valley load, and improve the efficiency of system operation [7]–[11]. However, the randomness of renewable energy output and the fluctuation of load set up difficulties for the operation of RIES.

The main problem in the RIES research is how to make the system operate flexibility and economically under the

The associate editor coordinating the review of this manuscript and approving it for publication was Zhouyang Ren[ID].

influence of multiple energy sources, thus stabilizing the randomness of the renewable energy output and the volatility of the load. In these solutions, IDR should be considered an effective method [12]. However, many studies only consider the demand response of the electric load in the RIES [13], ignoring the demand response of the natural gas load to improve the flexibility and reliability of the system operation, and do not consider the mutual substitution between different energy sources at the peak of energy use [14].

In order to realize the reasonable scheduling and reduce the operation cost of RIES, only study the day-ahead can not fully reflect the impact of the randomness of renewable energy and load on the system [15]–[18]. On the one hand, the existing research mainly focuses on the analysis of energy scheduling time of multi-energy coupling and multi-time scale scheduling. Reference [19] establish a RIES joint scheduling model with renewable energy, CCHP and energy storage systems, and finally the model is solved by Cplex. Reference [20], [21] considering the constraints of multiple
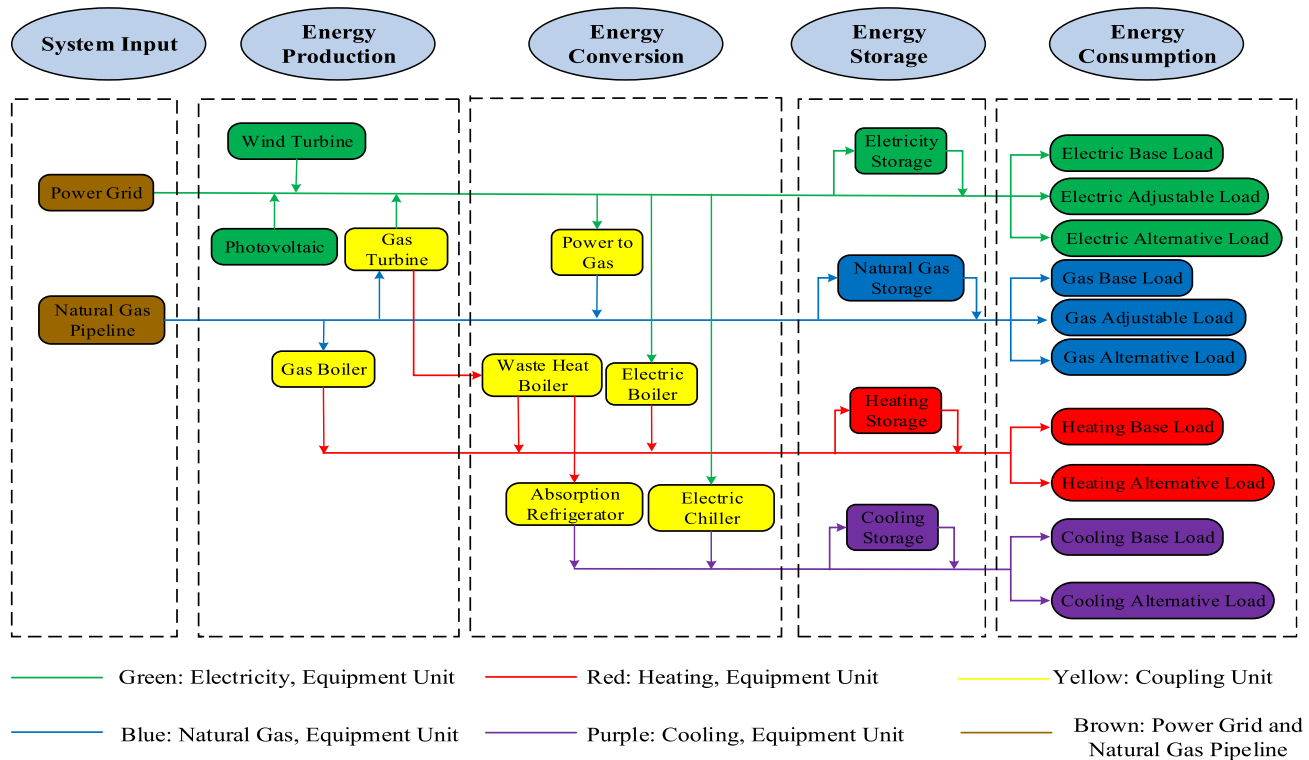
FIGURE 1. Structure diagram of RIES.

types of power generation and energy storage, an operation optimization model with renewable energy and multiple energy demands is established to realize the comprehensive utilization and collaborative optimization of multiple energy flows.

On the other hand, few studies have been made on the different energy scheduling time. Reference [22] based on the model predictive control, a multi-time scale optimal scheduling strategy is proposed to carry out multi-time period rolling optimization intraday. Reference [23] proposing a multi-time scale optimal scheduling model of CCHP microgrid, which optimizes the intraday cooling/ heating and electric energy respectively, making the system more stable and economical. Reference [24] considering the uncertainty of both source and load resources, the paper introduces price and incentive demand response, and establishes the source load interaction model of the day-ahead and intraday.

The main contributions of this paper are as follows:

1) Establish a multi-time scale model of RIES considering IDR, including electric, cooling/heating and natural gas energy system, and realize multi-energy system scheduling and optimization through energy coupling equipment and energy storage equipment.

2) Proposing an IDR model includes price-based and alternative response. The former represents the transfer effect of the same kind of energy demand at different time nodes based on price guidance, while the latter

represents the substitution effect of different energy demand at the same time node.

3) Proposing a method for intraday rolling optimization scheduling. Considering the difference of electric, cooling/heating and natural gas energy scheduling time, the intraday optimal scheduling model is divided into three different control layers for optimal scheduling.

The remaining of this paper is organized as follows, the architecture of the RIES model is introduced in Section II. the IDR model is introduced in Section III, and Section IV establishes the RIES multi-time scale optimization scheduling model considering the comprehensive demand response. Case studies are conducted in Section V to proves the validity of the proposed model. Section VI gives the final conclusion.

II. STRUCTURE DIAGRAM OF RIES

The structure of the RIES in this paper is illustrated in Fig. 1. Generally, RIES can be divided into five parts: system input, energy production, energy conversion, energy storage and energy consumption.

The system receives power from the superior grid and natural gas from the outside.

Energy production includes various distributed power generation devices such as gas turbine (GT), gas boiler (GB), wind turbine (WT) and photovoltaic (PV) power generation devices. This part mainly uses primary energy such as natural

gas and solar energy to produce electric energy and thermal energy required by users.

Energy conversion includes power-to-gas (PtG), waste heat boiler (WHB), absorption refrigerator (AR), electric chiller (EC) and electric boiler (EB). In this part, different forms of energy are converted to make different energy flows connect with each other and meet the diversified energy needs of users. Energy conversion generally follows the rule of transforming from high-grade energy to low-grade energy, and the taste of electricity, heating and cooling energy gradually decreases. Therefore, the input of the energy conversion unit is generally electricity and heating, while the output is generally heating and cooling.

Energy storage includes electricity storage (ES), gas storage (GS), heat storage (HS) and cold storage (CS). This part can fully absorb the system capacity, realize the cross period transfer of energy, balance the load, cut the peak and fill the valley.

Energy consumption is the user of the system terminal. The energy demand of users is usually four kinds: electricity, natural gas, heating and cooling. The electricity demand is various office and household appliances, motors and electric vehicles; the natural gas demand is household cooking and natural gas vehicles; the heating/cooling demand is heating in winter and cooling in summer.

III. IDR MODEL

The introduction of IDR can change the user's energy consumption behavior curve, reduce the system operation cost and improve the system operation efficiency. In this paper, the system load is divided into traditional load and energy coupling load. According to the price sensitivity, the traditional load can be divided into two types: the fixed load which is not affected by the demand side response mode and the price-based load which is affected by the price fluctuation. The energy coupling load can be replaced by other energy sources to achieve the same energy use effect. In order to reduce the complexity of the model, this paper does not consider the effect of alternative load on price response.

A. PRICE-BASED DEMAND RESPONSE
The widely used elasticity matrix of electricity price is used to solve the demand side electricity load, and the elasticity coefficient of electricity price is obtained by comparing the electricity consumption with the corresponding price change:

$$\eta = \frac{\Delta q}{\Delta p} \cdot \frac{p}{q} \tag{1}$$

where η is elastic coefficient of electricity price, Δq is the relative increase of electricity quantity q, Δp is the relative increase of electricity price q.

The above self elasticity coefficient represents the response of electricity to the change of electricity price at that time, and the cross elasticity coefficient represents the response of electricity to the change of electricity price in other time.

$$\eta_{aa} = \frac{\Delta q_a}{\Delta p_a} \cdot \frac{p_a}{q_a} \tag{2}$$

$$\eta_{ab} = \frac{\Delta q_a}{\Delta p_b} \cdot \frac{p_b}{q_a} \tag{3}$$

where a, b represents different time periods.

Therefore, for period $1 \sim n$ there is the following relationship.

$$\left[\frac{\Delta q_1}{q_1} \frac{\Delta q_2}{q_2} \cdots \frac{\Delta q_n}{q_n}\right]^{\mathrm{T}} = E_e \left[\frac{\Delta p_1}{p_1} \frac{\Delta p_2}{p_2} \cdots \frac{\Delta p_n}{p_n}\right]^{\mathrm{T}} \tag{4}$$

$$E_e = \begin{bmatrix} \eta_{11} & \eta_{12} & \cdots & \eta_{1n} \\ \eta_{21} & \eta_{22} & \cdots & \eta_{2n} \\ \vdots & \vdots & \vdots & \\ \eta_{n1} & \eta_{n2} & \cdots & \eta_{nn} \end{bmatrix} \tag{5}$$

where E_e is the elasticity matrix of electricity price.

The total electric quantity after the demand side response is calculated as follows:

$$q_z = q_n + \Delta q_n = [q_1 \cdots q_n] \\ + [q_1 \cdots q_n] E_d \left[\frac{\Delta p_1}{p_1} \cdots \frac{\Delta p_n}{p_n}\right]^{\mathrm{T}} \tag{6}$$

where q_z is total electric quantity after the demand side response, q_n refers to the load quantity in n period before demand side response and Δq_n is the change value of load quantity in n period after demand side response.

Considering that natural gas has the same commodity attribute as electric energy, the method of calculating natural gas load is obtained by analogy with the time-sharing price method of electric load above. The elasticity coefficient of natural gas is as follows:

$$\omega = \frac{\Delta g}{\Delta r} \cdot \frac{r}{g} \tag{7}$$

where ω is elastic coefficient of electricity price, Δg is the relative increase of electricity quantity g, Δr is the relative increase of electricity price r.

The natural gas self elasticity coefficient and cross elasticity coefficient are as follows:

$$\omega_{aa} = \frac{\Delta g_a}{\Delta r_a} \cdot \frac{r_a}{g_a} \tag{8}$$

$$\omega_{ab} = \frac{\Delta g_a}{\Delta r_b} \cdot \frac{r_b}{g_a} \tag{9}$$

Therefore, for period $1 \sim n$ there is the following relationship.

$$\left[\frac{\Delta g_1}{g_1} \cdots \frac{\Delta g_n}{g_n}\right]^{\mathrm{T}} = E_g \left[\frac{\Delta r_1}{r_1} \cdots \frac{\Delta r_n}{r_n}\right]^{\mathrm{T}} \tag{10}$$

$$E_g = \begin{bmatrix} \omega_{11} & \omega_{12} & \cdots & \omega_{1n} \\ \omega_{21} & \omega_{22} & \cdots & \omega_{2n} \\ \vdots & \vdots & \vdots & \\ \omega_{n1} & \omega_{n2} & \cdots & \omega_{nn} \end{bmatrix} \tag{11}$$

where E_g is the elasticity matrix of electricity price.

TABLE 1. Applicable loads of different demand side responses.

Type	Fixed type	Price type	Alternative type
Electric load	Fixed electrical load in traditional users	Time-shifting electrical load in traditional users	
Natural gas loading	Fixed gas load in traditional users	Time-shifting gas load in traditional users	Electric, natural gas and cooling/heating loads in energy coupling
Cooling/ heating load	—— ——	—— ——	

The total amount of natural gas after demand side response is as follows:

$$g_z = g_n + \Delta g_n = [g_1 \cdots g_n] E_q \left[\frac{\Delta r_1}{r_1} \cdots \frac{\Delta r_n}{r_n} \right] \quad (12)$$

where g_z is total natural gas quantity after the demand side response, g_n refers to the load quantity in n period before demand side response and Δg_n is the change value of load quantity in n period after demand side response.

B. ALTERNATIVE DEMAND RESPONSE

In RIES, energy sources such as electricity, natural gas and cooling / heating energy are transferred between different energy sources through related coupling equipment. Users can use other energy to replace the required energy, so that the system can operate more stably and improve the efficiency of energy utilization. Therefore, the alternative demand response based on the coupling of multi-energy sources is applied. The energy conversion follows the law of conservation of energy, and the transformation relationship of alternative demand response is as follows:

$$\Delta R_i = -\gamma_{i,j} \Delta R_j \quad (13)$$

$$\gamma_{i,j} = \frac{W_i \cdot \eta_i}{W_j \cdot \eta_j} \quad (14)$$

$$\Delta R_i^{\min} \leq \Delta R_i \leq \Delta R_i^{\max} \quad (15)$$

$$\Delta R_j^{\min} \leq \Delta R_j \leq \Delta R_j^{\max} \quad (16)$$

where i, j respectively represent two kinds of energy sources, such as electricity, natural gas, cold and heat, ΔR_i, ΔR_j respectively represent the load increment of a certain two kinds of energy sources, $\gamma_{i,j}$ is the conversion coefficient between energy sources, W_i, W_j respectively are the unit calorific value of energy sources i and j, η_i, η_j respectively are the utilization ratio of energy sources i and j, $\Delta R_i^{\min}$, $\Delta R_j^{\min}$ respectively are the minimum values of energy sources i and j load increments, $\Delta R_i^{\max}$, $\Delta R_j^{\max}$ respectively are the maximum values of energy sources i and j load increments.

The responsive electrical, natural gas, cooling/heating alternative loads are obtained from:

$$L_i = L_i^0 + \Delta L_i \quad (17)$$

where L_i^0 represents the alternative load before response, ΔL_i represents the change amount of load response.

In order to ensure that the load does not increase or decrease in the above system and meet the user's requirements, the load conversion balance constraint is introduced.

$$\sum_{i=1}^{N} \Delta L_i = 0 \quad (18)$$

where N represents a collection of all types of energy in the energy coupling.

IV. MULTI-TIME SCALE OPTIMAL SCHEDULING MODEL OF RIES CONSIDERING IDR

In this paper, a multi-time scale optimal operation model is proposed, including day-ahead dispatching and intraday rolling optimal operation. Intraday rolling optimal operation is divided into three sublayer according to energy characteristics [25].

A. DAY-AHEAD SCHEDULING

1) OBJECTIVE FUNCTION

The day-ahead scheduling is based on the minimum cost of scheduling as the objective function to formulate the next day scheduling plan.

$$\min F = F_e + F_g + F_p \quad (19)$$

where F_e is the electrical power purchase cost, F_g is natural gas purchase cost, F_p is equipment maintenance cost during the scheduling period.

Electricity purchasing cost is as follows:

$$F_e = \sum_{T=1}^{24} \left(\frac{C_{rs}^T + C_{rb}^T}{2} P_{grid}^T + \frac{C_{rb}^T - C_{rs}^T}{2} \left| P_{grid}^T \right| \right) \quad (20)$$

where P_{grid}^T is the RIES and grid interactive power at time T, C_{rs}^T is the electrical power purchasing price at time T, C_{rb}^T is the electrical power selling price at time T.

Cost of purchasing natural gas is as follows:

$$F_g = \sum_{T=1}^{24} \left(F_{source}^T C_{gas} \right) \quad (21)$$

where F_{source}^T is represents the natural gas purchased at time T, C_{gas} is the natural gas purchasing price at time T.

Maintenance cost of equipment during operation is as follows:

$$F_p = \sum_{T=1}^{24} \left(\sum_{d=1}^{N} C_b \left| P_b^T \right| \right) \tag{22}$$

where b is the unit equipment, C_b is represents the unit maintenance cost, P_b^T is the output power at the time T.

2) CONSTRAINTS

a: ENERGY SUPPLY AND EDMAND BALANCE CONSTRAINTS

The electrical energy supply and demand balance equation is as follows:

$$P_{WT}^T + P_{PV}^T + P_{grid}^T + P_{GT}^T + P_{ES}^T = P_{Dmd}^T + P_o^T \tag{23}$$

where P_{WT}^T is the electric power generated by WT at the time T, P_{PV}^T is the electric power generated by PV at the time T, P_{grid}^T is the purchased electrical power at the time T, P_{GT}^T is the electric power generated by GT at the time T, P_{ES}^T is the output value of ES; P_{Dmd}^T is the total load power on the demand side, P_o^T is the electric power consumed by coupling equipment.The natural gas energy supply and demand balance equation is as follows:

$$G_{PtG}^T + G_{source}^T + G_{GS}^T = G_{Dmd}^T + G_o^T \tag{24}$$

where G_{PtG}^T is the natural gas generated by PtG at the time T, G_{source}^T is the purchased natural gas at the time T, G_{GS}^T is the output value of GS, G_{Dmd}^T is the total natural gas load on the demand side, G_o^T is the natural gas consumed by coupling equipment.

The cold energy supply and demand balance equation is as follows:

$$C_{EC}^T + C_{AR}^T + C_{CS}^T = C_{Dmd}^T \tag{25}$$

where C_{EC}^T is the cooling generated by EC at the time T, C_{AR}^T is the cooling generated by AR at the time T, C_{CS}^T is the output value of CS, C_{Dmd}^T is the total cooling load on the demand side.

The thermal energy supply and demand balance equation is as follows:

$$H_{GB}^T + H_{EB}^T + H_{WHB}^T + H_{HS}^T = H_{Dmd}^T \tag{26}$$

where H_{GB}^T is the heating generated by GB at the time T, H_{WHB}^T is the heating generated by WHB at the time T, H_{EB}^T is the heat generated by EB at the time T, H_{HS}^T is the output value of HS, H_{Dmd}^T is the total heating load on the demand side.

b: CONSTRAINTS OF ENERGY CONVERSION DEVICES

$$P_b, \min \le P_b \le P_b, \max \tag{27}$$

where P_b is the output power, $P_{b,\min}/P_{b,\max}$ is the lower/upper limit of P_b.

c: CONSTRAINT OF RIES INTERACTION BETWEEN ELECTRICITY / NATURAL GAS NETWORK

$$P_{grid,ex}^{\min} \le P_{grid,ex} \le P_{grid,ex}^{\max} \tag{28}$$

$$G_{source,ex} \le G_{source,ex}^{\max} \tag{29}$$

where $P_{grid,ex}$ is power interaction values with electricity grid, $G_{source,ex}$ is interaction values with natural gas network, $P_{grid,ex}^{\min}/P_{grid,ex}^{\max}$ is the lower/upper limit of interaction values with electricity grid, $G_{source,ex}^{\max}$ is upper limits of interaction values with natural gas network.

d: CONSTRAINTS OF ENERGY STORAGE DEVICES

$$-C_{k,ES}^c P_{k,cp} \le C_{k,ES} \le C_{k,ES}^f P_{k,cp} \tag{30}$$

$$\lambda_{min} P_{k,cp} \le C_{k,cp}(t) \le \lambda_{max} P_{k,cp} \tag{31}$$

where $C_{k,ES}(t)$ is power of energy storage at time T, $C_{k,cp}(t)$ is capacity of energy storage at time T, $C_{k,ES}^c/C_{k,ES}^f$ is the discharge/discharging power ratio, $\lambda_{min}/\lambda_{max}$ is the lower/upper limit of state of charge, $C_{k,cp}$ is the maximum storage capacity of the energy storage equipment [26].

By using MATLAB software and the Cplex toolbox to solve the day-ahead scheduling model, the planned values of each coupled equipment operation and energy storage equipment charge/discharging are: [P_{GT}, P_{GB}, P_{WHB}, P_{EB}, P_{AR}, P_{EC}, P_{PtG}, S_{ES}, S_{CS}, S_{HS}, S_{GS}], and each coupled equipment operation and energy storage equipment operating status.

B. INTRADAY TIME-SCALE SCHEDULING

The intraday rolling optimization scheduling is divided into three control sublayers: the slow control sublayer, which is used to optimize the cooling/heating energy with a longer scheduling time, the control time domain k_1 is 1hours, and the scheduling time window is 2 hours; the intermediate control sublayer is used to optimize the long dispatch time of natural gas energy, the control time domain k_2 is 30 minutes, and the dispatch time window is 1 hours. The fast control sublayer is used to optimize the shorter dispatch time of power, the control time domain k_3 is 5 minutes, and the dispatch time window is 30 minutes [27].

As shown in Figure 2, at t_0 time, the system predicts that the cooling/heating energy $t_0 + 1$ to $t_0 + 3$ and adjust $t_0 + 1$ to $t_0 + 2$ the period power; the system predicts that the natural gas $t_0 + k_2$ to $t_0 + 1 + k_2$ and adjust $t_0 + k_2$ to $t_0 + 1$ the period power; and the system predicts that the electricity $t_0 + k_3$ to $t_0 + 1 + k_3$ and adjust $t_0 + k_3$ to $t_0 + 2k_3$ the period power.Due to the difference of scheduling time, the scheduling sequence is cooling/ heating, natural gas and electric energy.

1) SLOW LAYER ROLLING OPTIMAL SCHEDULING MODEL

Comply with the operating status of the GT and the cooling / heating energy scheduling strategy day-ahead, and adjust the output of each unit of the system according to the cooling / heating load change at time t. The objective function is as
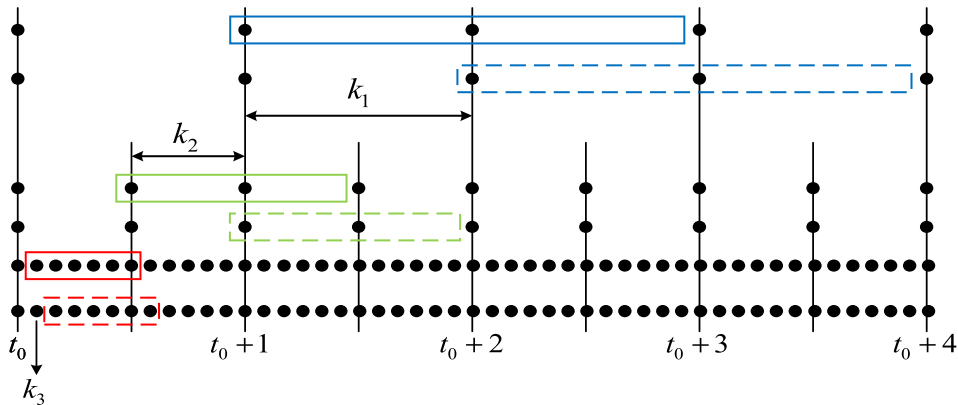
FIGURE 2. Optimized daily cooling / heating, natural gas and electric rolling scheduling.

follows:

$$F_1 = \min \sum_{t=k}^{k+k_1} \left(F_{g,1} + F_{e,1} \right) \quad (32)$$

Natural gas cost is as follows [23]:

$$F_{g,1} = \left[R_{gas}^t \left(F_{GT}^T + \Delta F_{GT}^t + F_{GB}^T + \Delta F_{GB}^t \right) \right. \\ \left. + \mu_{GT} \left(\Delta P_{GT}^t \right)^2 + \mu_{GB} \left(\Delta P_{GB}^t \right)^2 \right] \Delta t \quad (33)$$

where R_{gas}^t is the unit price of natural gas at time t, ΔF_{GT}^t is the consumption change of GT at time T, ΔF_{GB}^t is the consumption change of GB at time T, μ_{MT} is adjust the unit cost for GT, μ_{GB} is adjust the unit cost for GB, ΔP_{GT}^t is the adjustment power of GT at time t, ΔP_{GB}^t is the adjustment power of GB at time t, Δt is the unit time interval.

Changing costs of electric equipment is as follows:

$$F_{e,1} = \mu_{EB} \left(\Delta P_{EB} \right)^2 \Delta t + \mu_{EC} \left(\Delta P_{EC} \right)^2 \Delta t \quad (34)$$

where μ_{EB} is adjust the unit cost for EB, μ_{EC} is adjust the unit cost for EC, ΔP_{EB} is the adjustment power of EB at time t, ΔP_{EC} is the adjustment power of EC at time t.

The constraints of cooling/ heating supply and demand balance are shown in equation (25) and equation (26); the related coupling equipment is shown in equation (27).

2) INTERMEDIATE LAYER ROLLING OPTIMAL SCHEDULING MODE

Comply with the state of GS inhalation and degassing in day-ahead, and adjust the output of each unit of the system according to the natural gas load and slow control layer equipment changes during the period t. The objective function is as follows:

$$F_2 = \min \sum_{t=k}^{k+k_2} \left(F_{g,2} + F_{e,2} \right) \quad (35)$$

Cost of purchasing natural gas is as follows:

$$F_{g,2} = R_{gas}^t \left(G_{source}^T + \Delta G_{source}^t \right) \Delta t \quad (36)$$

where ΔG_{source}^t is the change of the interaction power between the natural gas network at time t.

Change cost of electric equipment is as follows:

$$F_{e,2} = \mu_{PtG} \left(\Delta P_{PtG}^t \right)^2 \Delta t \quad (37)$$

where μ_{PtG} is the unit adjustment cost of PtG, ΔP_{PtG}^t is the PtG adjustment power at time t.

The constraint of natural gas supply and demand balance is shown in equation (24), the constraint of interaction power with natural gas source is shown in equation (29).

3) FAST LAYER ROLLING OPTIMAL SCHEDULING MODE

Comply with the state of charge and discharge of the day-ahead, and modify the intraday scheduling according to the fluctuation of new energy and the power changes of the demand side and the above two sub-layers during the period t. The objective function is as follows:

$$F_3 = \min \sum_{t=k}^{k+k_3} \left(F_{e,3} + F_{ES} \right) \quad (38)$$

Cost of interaction with grid is as follows:

$$F_{e,3} = \left[\begin{array}{c} R_{grid}^t \left(P_{grid}^T + \Delta P_{grid}^t \right) + \\ \mu_{grid} \left(\Delta P_{grid}^t \right)^2 \end{array} \right] \Delta t \quad (39)$$

where R_{grid}^t is the electrical power purchasing price at time t, ΔP_{grid}^t is the change of the interactive power between the grid at time t, μ_{grid} is the unit adjustment cost of the interactive power.

Change cost of ES charging/discharging is as follows:

$$F_{ES} = \mu_{ES} \left[\left(\Delta P_c^t \right)^2 + \left(\Delta P_f^t \right)^2 \right] \Delta t \quad (40)$$

where μ_{ES} is ES unit adjustment cost, and $\Delta P_c^t / \Delta P_f^t$ is ES charging/discharging adjustment power at time t.

The constraints of power supply and demand balance are shown in equation (23); the constraints of power interaction with the grid are shown in equation (28).

TABLE 2. RIES operation parameters.

Type	P_{min} / kW	P_{max} / kW	Type	P_{min} / kW	P_{max} / kW
GT	15	60	AR	10	30
GB	0	50	WHB	10	35
EC	0	45	PtG	0	20
EB	0	50	Power grid	-80	80

TABLE 3. Peak valley TOU price.

Time	Time interval	Power purchase (yuan / (kWH))	Electricity sales (yuan/ (kWH))
Peak time	10:00-15:00 18:00-21:00	0.86	0.68
Flat time	07:00-10:00 15:00-18:00 21:00-23:00	0.61	0.50
Valley time	00:00-07:00 23:00-24:00	0.30	0.26

TABLE 4. Parameters of each energy storage system.

Parameter	Electrical energy storage	Gas energy storage	Cooling energy storage	Thermal energy storage
$C_{k,ES}^{c}$	0.25	0.25	0.25	0.25
$C_{k,ES}^{f}$	0.25	0.25	0.25	0.25
λ_{min}	0.2	0.1	0.1	0.1
λ_{max}	0.8	0.8	0.8	0.8
$P_{k,cp}$	150	150	100	100

C. DEMAND-SIDE RESPONSE STRATEGIES ON MULTI-TIME SCALES

During the day-ahead dispatching, the fixed loads in the traditional category and part of the electrical loads adjusted after the price-based response are initially fitted, and then the cooling/heating load values that are satisfied by the coupling equipment are determined [23].

During intraday rolling optimization, according to the day-ahead pre-scheduling plan, further consider the impact of demand-side fluctuations, and use alternative responses for hierarchical energy optimization.

V. SIMULATION ANALYSIS
A. EXAMPLE PARAMETER SETTING

In this paper, RIES of a certain region is selected for analysis, and the system structure is shown in Fig. 1.The self elasticity coefficient of electricity price is −0.2, cross elasticity coefficient is 0.03; the self elasticity coefficient of time-sharing price type natural gas is −0.58, cross elasticity coefficient is 0.15.In the calculation example, the operation parameters of

RIES are shown in Table 2, the time-of-use (TOU) price of peak and valley is shown in Table 3, the parameters of each energy storage system are shown in Table 4, and the load and scenery prediction curve is shown in Fig. 3.

B. COMPARISON OF DIFFERENT SCHEDULING MODELS

Model 1: Day-ahead scheduling plan considering only price-based demand response.

Model 2: Day-ahead scheduling plan considering price-based and alternative demand response.

Model3: Considering the day-ahead and intraday scheduling plans of price-based and alternative response, the intraday scheduling plan model does not optimize electric cooling / heating and natural gas energy in layers.

Model 4: the model proposed in this paper.

Compared with the running cost of the scheduling model proposed in this paper, as shown in Table 5. In Model 1, because cooling/heating energy is supplied internally by the system, price-type demand response cannot be applied, that is, the demand response of cooling/heating energy is not
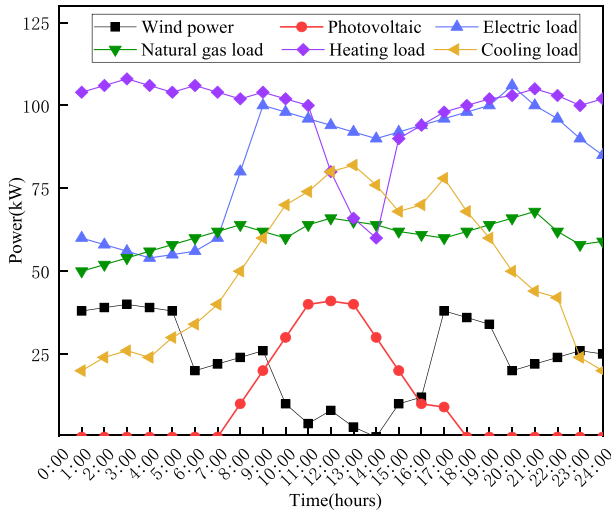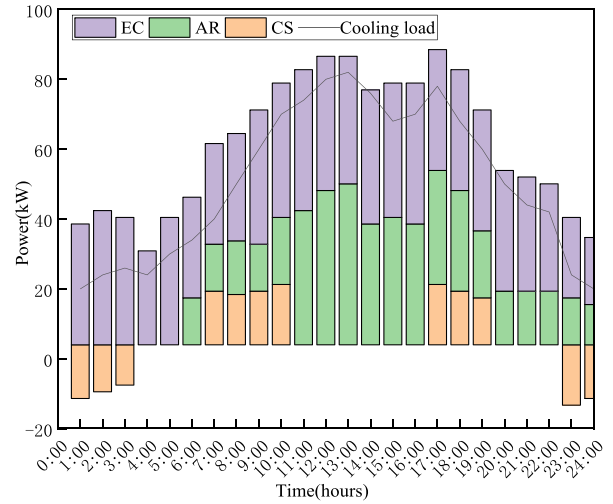
FIGURE 3. Load and scenery prediction curve.
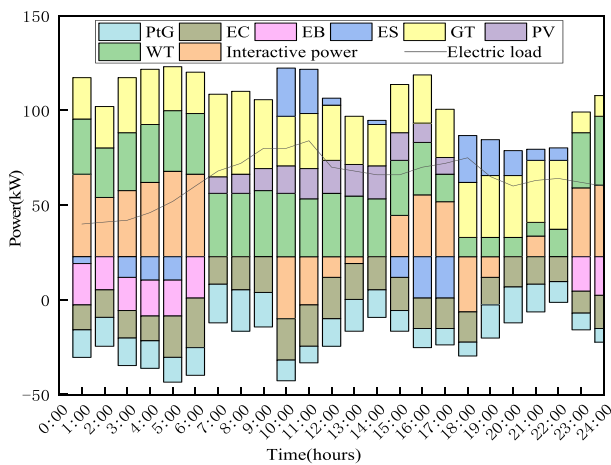

FIGURE 4. Power supply and demand balance.

FIGURE 5. Balance of natural gas supply and demand.

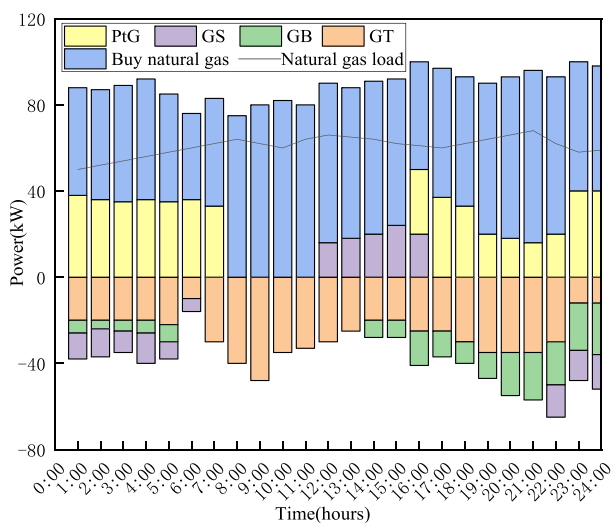

FIGURE 6. Supply and demand balance of cold energy.

FIGURE 7. Balance of heat supply and demand.

considered, so the scheduling cost is higher in this model; Model 2 only considers day-ahead scheduling and cannot stabilize intraday renewable energy and load fluctuate, so the

scheduling cost under this model will also become higher, the total daily cost of Model 1 is 58625 yuan, and the total daily cost of Model 2 is 57429 yuan. The total daily cost of Model 2 is 2.04% lower than the total daily cost of Model 1, and the abandonment and light are reduced by 0.8%; In the day-ahead and intraday model of Model 3, the intraday model does not take into account the differences in electricity, cooling/heating, and natural gas scheduling time, and Model 4 is based on Model 3, in which the intraday model takes into account the differences of electricity, cooling/ heating and natural gas scheduling time, which can better suppress the fluctuations of both sides of supply and demand, and ensure the stable operation of the system and the external power grid. Therefore, compared with Model 3, Model 4 reduced electricity purchase by 1.61%, natural gas purchase by 1.22%, and abandoned wind and light by 1.4%.

C. DAILY SCHEDULING ANALYSIS

As shown in Fig. 4 to Fig. 7, under the condition of mutual coupling of electric, cooling/heating and natural gas network,
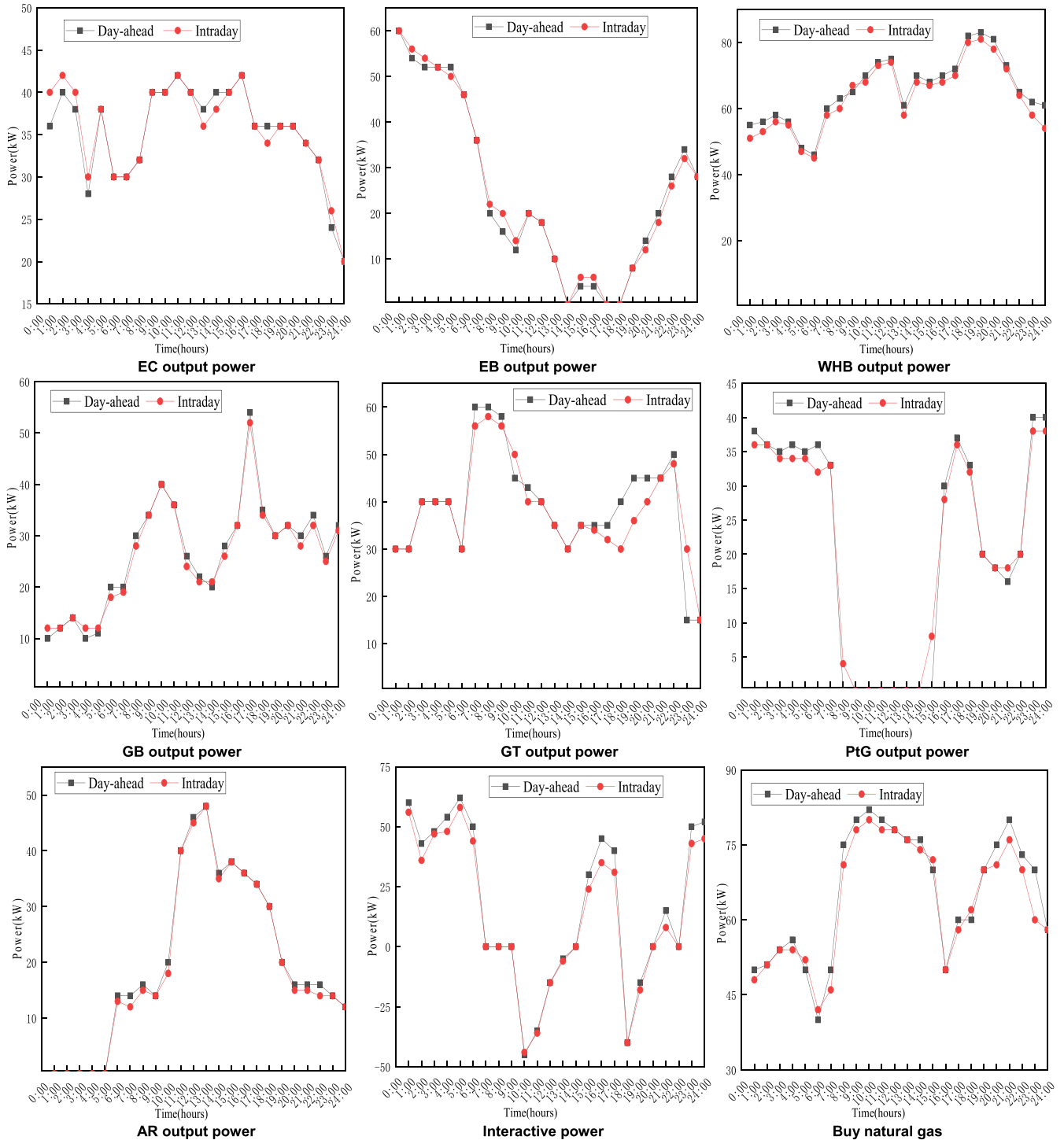
FIGURE 8. Multi-time scale optimization results.

the system can meet the balance of supply and demand. During the period from 23:00 to 07:00 of the next day, the electricity price is at a low level.The system will guide the electric energy to be converted into thermal energy through EB and give priority to output; guide the electric energy to be converted into natural gas through PtG device to increase

the output of PtG; guide the electric energy to be converted into cold energy through EC equipment to meet the cooling load.When the electricity price is in the peak period.GT increases output to replace the interactive power with power generation, and increases the discharge capacity of ES to meet the demand of electric energy, such as period 18:00 to 20:00;

TABLE 5. Operation costs of different scheduling models.

Scheduling model type	Total operation cost (yuan)	Power purchase cost (yuan)	Cost of purchasing natural gas(yuan)	Abandon wind and light (%)
1	58625	32796	15829	8
2	57429	31923	15506	7.2
3	56925	31555	15370	6.6
4	56225	31044	15181	5.2

it will also guide PtG to reduce output, such as period 10:00 to 14:00; cooling load mainly depends on AR to meet the demand, such as period 10:00 to 15:00; heating load mainly depends on WHB to meet the demand, such as period 18:00 to 21:00.When the electricity price is in the normal period.The load is reduced, and HS releases heating to reduce GT output, such as 21:00 to 23:00; AR output tends to reduce, and natural gas demand is reduced, such as 07:00 to 10:00.

D. ANALYSIS OF ROLLING OPTIMAL SCHEDULING INTRADAY

The results of the day-ahead and intraday optimal scheduling are shown in Figure 8. Based on the day-ahead scheduling, the output of the coupling equipment and the interaction power with the external network are corrected within intraday. Compared with the day-ahead, the purchase of electricity and natural gas was reduced intraday. The reduction of electricity purchase 45 kWH and natural gas purchase 37m^3 during the day can save 120 yuan in energy purchase costs.The interactive power curve with the power grid fluctuates with the change of electricity price, and the power purchase is significantly reduced in the peak period, so as to achieve better economic performance. When the electricity price is high, let GT run to generate electricity to keep the balance of supply and demand of the system. The natural gas and cooling/heating are also optimized more accurately, and the output of coupling equipment will also change.

VI. CONCLUSION

Based on the characteristics of price-based and alternative responses, this paper considers the differences in scheduling time of electricity, cooling/heating, and natural gas, and proposes an RIES multi-time scale optimal scheduling model that takes into account the demand-side response. The following conclusions are obtained:

(1) Demand-side response is related to the efficiency of RIES's dispatch operation. When the system is dispatched according to the model proposed in this paper, its economic operation cost is optimal and it can better reflect the advantages of demand-side response.

(2) The RIES is optimized for multiple time scales. Based on the results of the day-ahead optimization, the time scale is further shortened within intraday to improve the accuracy of the system decision.

(3) A three-layer rolling optimization scheduling model within the day can dispatch electricity, cooling/heating, and natural gas on different time scales separately, so that the system can suppress the fluctuations of the supply and demand sides and ensure the stable operation of the system.

REFERENCES

[1] G. Bridge, B. Özkaynak, and E. Turhan, "Energy infrastructure and the fate of the nation: Introduction to special issue," *Energy Res. Social Sci.*, vol. 41, pp. 1–11, Jul. 2018.

[2] H. Lund, A. N. Andersen, P. A. Østergaard, B. V. Mathiesen, and D. Connolly, "From electricity smart grids to smart energy systems—A market operation based approach and understanding," *Energy*, vol. 42, no. 1, pp. 96–102, Jun. 2012.

[3] J. Yu, H. Sun, and X. Shen, "Optimal operating strategy of integrated power system with wind farm CHP unit and heat storage device," *Electr. Power Automat. Equip.*, vol. 37, no. 6, pp. 139–145, 2017.

[4] P. Palensky, E. Widl, and A. Elsheikh, "Simulating cyber-physical energy systems: Challenges, tools and methods," *IEEE Trans. Syst., Man, Cybern. Syst.*, vol. 44, no. 3, pp. 318–326, Mar. 2014.

[5] M. Moeini-Aghtaie, A. Abbaspour, M. Fotuhi-Firuzabad, and P. Dehghanian, "Optimized probabilistic PHEVs demand management in the context of energy hubs," *IEEE Trans. Power Del.*, vol. 30, no. 2, pp. 996–1006, Apr. 2015.

[6] A. Pini Prato, F. Strobino, M. Broccardo, and L. Parodi Giusino, "Integrated management of cogeneration plants and district heating networks," *Appl. Energy*, vol. 97, pp. 590–600, Sep. 2012.

[7] S. Moslehi and T. A. Reddy, "Sustainability of integrated energy systems: A performance-based resilience assessment methodology," *Appl. Energy*, vol. 228, pp. 487–498, Oct. 2018.

[8] Y. Wang, H. Yu, M. Yong, Y. Huang, F. Zhang, and X. Wang, "Optimal scheduling of integrated energy systems with combined heat and power generation, photovoltaic and energy storage considering battery lifetime loss," *Energies*, vol. 11, no. 7, p. 1676, Jun. 2018.

[9] W. Xiong, Y. Wang, B. V. Mathiesen, H. Lund, and X. Zhang, "Heat roadmap China: New heat strategy to reduce energy consumption towards 2030," *Energy*, vol. 81, pp. 274–285, Mar. 2015.

[10] A. Navidi and F. A.-S. Khatami, "Energy management and planning in smart cities," *CIRED-Open Access Proc. J.*, vol. 2017, no. 1, pp. 2723–2725, Oct. 2017.

[11] K. Difs and L. Trygg, "Pricing district heating by marginal cost," *Energy Policy*, vol. 37, no. 2, pp. 606–616, Feb. 2009.

[12] Z. Jiang, Q. Ai, and R. Hao, "Integrated demand response mechanism for industrial energy system based on multi-energy interaction," *IEEE Access*, vol. 7, pp. 66336–66346, 2019.

[13] M. F. Tahir, C. Haoyong, K. Mehmood, N. Ali, and J. A. Bhutto, "Integrated energy system modeling of china for 2020 by incorporating demand response, heat pump and thermal storage," *IEEE Access*, vol. 7, pp. 40095–40108, 2019.

[14] P. Jie, Z. Tian, S. Yuan, and N. Zhu, "Modeling the dynamic characteristics of a district heating network," *Energy*, vol. 39, no. 1, pp. 126–134, Mar. 2012.

[15] X. Zhang, M. Shahidehpour, A. Alabdulwahab, and A. Abusorrah, "Optimal expansion planning of energy hub with multiple energy infrastructures," *IEEE Trans. Smart Grid*, vol. 6, no. 5, pp. 2302–2311, Sep. 2015.

[16] F. Dong, Y. Hua, and B. Yu, "Peak carbon emissions in China: Status, key factors and countermeasures—A literature review," *Sustainability*, vol. 10, no. 8, p. 2895, Aug. 2018.

[17] L. Suganthi and A. A. Samuel, "Energy models for demand forecasting-A review," *Renew. Sustain. Energy Rev.*, vol. 16, no. 2, pp. 1223–1240, 2012.

[18] H. Aki, "Demand-side resiliency and electricity continuity: Experiences and lessons learned in Japan," *Proc. IEEE*, vol. 105, no. 7, pp. 1443–1455, Jul. 2017.

[19] H. Cho, P. J. Mago, R. Luck, and L. M. Chamra, "Evaluation of CCHP systems performance based on operational cost, primary energy consumption, and carbon dioxide emission by utilizing an optimal operation scheme," *Appl. Energy*, vol. 86, no. 12, pp. 2540–2549, Dec. 2009.

[20] B. Awad, M. Chaudry, J. Wu, and N. Jenkins, "Integrated optimal power flow for electric power and heat in a microgrid," in *Proc. CIRED IET*, 2009, pp. 1–4.

[21] A. Ehsan and Q. Yang, "Scenario-based investment planning of isolated multi-energy microgrids considering electricity, heating and cooling demand," *Appl. Energy*, vol. 235, pp. 1277–1288, Feb. 2019.

[22] A. Kargarian and G. Hug, "Optimal sizing of energy storage systems: A combination of hourly and intra-hour time perspectives," *IET Gener., Transmiss. Distrib.*, vol. 10, no. 3, pp. 594–600, Feb. 2016.

[23] Q. Jiang and H. Wang, "Two-time-scale coordination control for a battery energy storage system to mitigate wind power fluctuations," *IEEE Trans. Energy Convers.*, vol. 28, no. 1, pp. 52–61, Mar. 2013.

[24] G. Geng, V. Ajjarapu, and Q. Jiang, "A hybrid dynamic optimization approach for stability constrained optimal power flow," *IEEE Trans. Power Syst.*, vol. 29, no. 5, pp. 2138–2149, Sep. 2014.

[25] H. Wu, M. Shahidehpour, Z. Li, and W. Tian, "Chance-constrained day-ahead scheduling in stochastic power system operation," *IEEE Trans. Power Syst.*, vol. 29, no. 4, pp. 1583–1591, Jul. 2014.

[26] Y. Cao, S. Tang, C. Li, P. Zhang, Y. Tan, Z. Zhang, and J. Li, "An optimized EV charging model considering TOU price and SOC curve," *IEEE Trans. Smart Grid*, vol. 3, no. 1, pp. 388–393, Mar. 2012.

[27] Z. Zhou, P. Liu, Z. Li, and W. Ni, "An engineering approach to the optimal design of distributed energy systems in China," *Appl. Thermal Eng.*, vol. 53, no. 2, pp. 387–396, May 2013.

MENGLONG LI received the B.S. degree in electrical engineering from Henan Polytechnic University, Jiaozuo, China, in 2018, where he is currently pursuing the M.S. degree in electrical engineering.

His main research interests include smart grids, integrated energy systems, and demand response.

ZHAOYANG JIANG received the B.S. degree in electrical engineering from Henan Polytechnic University, Jiaozuo, China, in 2018, where he is currently pursuing the M.S. degree in electrical engineering.

His main research interests include regional integrated energy system planning, renewable energy, and smart grids.

HAIZHU YANG received the B.S. and M.S. degrees in electrical engineering from Henan Polytechnic University, Jiaozuo, China, in 1998 and 2002, respectively, and the Ph.D. degree in electrical engineering from Beijing Jiaotong University, Beijing, China, in 2005.

Since 2006, he has been with the School of Electrical Engineering and Automation, Henan Polytechnic University, where he is currently an Associate Professor. His research interests include power quality analysis and control, power electronics, and power transmission.

PENG ZHANG received the B.S. and M.S. degrees in electrical engineering from Tianjin University, Tianjin, China, in 2007 and 2010, respectively, and the Ph.D. degree in power electronics engineering from Kyushu University, Fukuoka, Japan, in 2013.

Since 2014, he has been with the School of Electrical and Information Engineering, Tianjin University, where he is currently a Lecturer. His research interests include integrated energy systems and microgrid energy management systems.

• • •